

OBSERVATIONS OF SEDIMENT PARTICLE MOVEMENTS DURING A STORM

Takayuki Suzuki¹, Yu Inami², Masayuki Banno³ and Yoshiaki Kuriyama⁴

Abstract

Field experiments were conducted on the Hasaki Coast of Japan facing the Pacific Ocean to observe sediment particle movements during a storm event. The objective of these experiments was to investigate cross-shore and vertical movements of sediment in the area from the swash zone to the offshore end of the surf zone. Five different colored fluorescent sand tracers were installed onto the seabed at five different locations, and eight vertical sand cores were collected for analysis after the storm. The analyzed results suggest that sand movements can be characterized differently for the onshore and offshore sides of the bar. Furthermore, the seabed profile data generated from the analyzed sand cores shows that sediment erosion and accumulation processes that occur during storm events are different, even when similar thicknesses of sediment accumulation has been detected, depending on the location.

Key words: morphodynamics, storm event, fluorescent sand tracers, core sampling, field experiment

1. Introduction

In the swash and surf zones of coastal regions, sediments move dynamically due to waves and currents, especially during storm events. Sediment Morphodynamics in these zones have been investigated by many researchers using results from field observations and laboratory analysis. Sediment dynamics have not only been observed using instruments to collect seabed profile data but also by conducting laboratory analysis of seabed sediment particle size distribution, core sampling and the distribution of fluorescent sand tracers. For example, Katoh and Yanagishima (1995) investigated the change in grain size distribution in a surf zone before and after a storm event. They reported a cyclic transportation of sediment with movement between the step, trough and bar areas. Kaczmarek et al. (2004) proposed a model of intensive cross-shore sand transportation and changes to the grain size distribution of a seabed.

Fluorescent sand tracers have also been used since the 1960s to investigate sediment transport dynamics, both for cross-shore and longshore sediment transport (e.g., Jolliffe, 1963; Kennedy, and Kouba, 1970). Later, Katoh and Tanaka (1986) used fluorescent tracers to investigate the localized sediment motion in the surf zone and Tonk and Masselink (2005) attempted to develop empirical equations for evaluating longshore sediment transport using data observed by fluorescent tracers and other instruments. Tracers have also been analyzed in laboratories to developed improved understanding of sediment transport and vertical mixing (e.g., Kraus and Smith, 1994; Williams et al., 2012).

Sediment in the surf and swash zones are mixed vertically due to the effects of waves and currents. Core sampling is frequently used to analyze sediment dynamics such as vertical mixing, bed accumulation, and erosion processes (e.g., Inman et al., 1980; Ciavola et al., 1997; Masselink et al., 2007). Moreover, Yamada et al. (2013) have applied medical X-ray methods such as computed tomography (CT) scanning to measure the dynamics of the seabed profile including sediment structures and transport processes in response to wave motions.

The majority of sediment related researches have focused on a limited region of the coastal area and studied the correlation between waves, currents, and sediment movements. There are few examples of research that investigates the phenomena of sediment transport and vertical mixing in the area from the

¹ Faculty of Urban Innovation, Civil Eng. Dept., Yokohama National University, Japan. suzuki-t@ynu.ac.jp

² Researcher, Civil Engineering Research Institute for Cold Region, Japan. inami-yuu-zc@ynu.jp

³ Senior researcher, Port and Airport Research Institute, Japan. banno-m@pari.go.jp

⁴ President, Port and Airport Research Institute, Japan. kuriyama@pari.go.jp

swash zone to the offshore side of the surf zone. This research examines this target area conducting field observations during a storm event. It combines data about the seabed profile with analyzed data from fluorescent sand tracers and core sampling to investigate both cross-shore and vertical movements of sediment.

2. Data Description

2.1. Hasaki Oceanographical Research Station, HORS

Field observations were conducted at the Hazaki Oceanographical Research Station (HORS), which is a research facility capable of field measurements of various phenomena in the nearshore zone of the Hasaki coast of Japan facing the Pacific Ocean (Fig. 1). The HORS has a 427-meter-long pier, which is perpendicular to the shoreline. The cross-shore distance along the pier is defined relative to the station as a reference point, which is located near the entrance of the pier. The seaward direction, x , is set as positive.

The average particle diameter of sediment along the pier has been reported to be approximately 0.18 mm (Kato et al., 1990). The Hasaki coast is relatively stable and the bathymetry surrounding the HORS has been found to be close to uniform along the shore (Kuriyama, 2002). The high, mean and low water levels based on the datum level at the Hasaki coast (Tokyo peil -0.687 m) are 1.25 m, 0.65 m, and -0.20 m, respectively.

Wave data at a cross-shore distance of $x = 303$ m were observed by using a wave gauge (UH-401, KENEK). Values for the significant wave height and significant wave period were calculated by recording a 20-minute data sample. Offshore waves were observed at a water depth of 23.4 m offshore the Kashima Port, which is located approximately 8 km north of the HORS. The significant wave height, wave period and wave direction was also observed at this site.

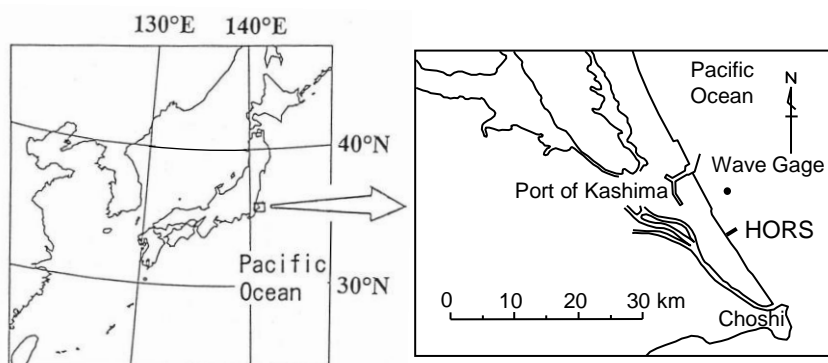


Figure 1. Location of Hazaki Oceanographical Research Station (HORS).

2.2. Outline of field experiments

Field observations were conducted for 12 days from October 19, 2014, to October 30, 2014, at the HORS. During this period, seabed profile surveys were conducted on four occasions as shown in Fig. 2. The profile along the pier was measured at 5 m intervals using a 3 kg lead and a level staff and automatic level landward of the pier. The bar, which was located at approximately $x = 260$ m at the start of the observation, was found to have moved offshore by approximately 25 m due to the storm event.

Five different colored fluorescent sand tracers, Picture 1, were installed on the seabed at five different locations from the swash zone to the offshore side of the bar ($x = 65$ m for pink, $x = 115$ m for yellow, $x = 180$ m for blue, $x = 240$ m for green, and $x = 290$ m for red) as shown in Fig. 2. The median diameter of the tracer particles was 0.2 mm, which is approximately the same diameter as Hazaki coastal sand. At each location, 225 kg of fluorescent sand was installed on the seabed by divers. A wave gauge and current meter were attached to an observation array that was installed near the bar at $x = 245$ m. (Fig. 2).

The significant wave height and significant wave period were observed at $x = 303$ m, as shown in Fig. 3.

Offshore wave direction was observed and recorded as a positive angle of a clockwise rotation, where zero degrees denotes the direction parallel to the pier from offshore to onshore. Three days after the installation of fluorescent sand tracers, a storm event occurred with wave heights of over 2 m. The offshore bar was observed to have moved further offshore by a distance of approximately 25 m (Fig. 2). To assess the impact of the storm on the seabed profile eight vertical sand cores were collected on October 30 at the end of the observation period.

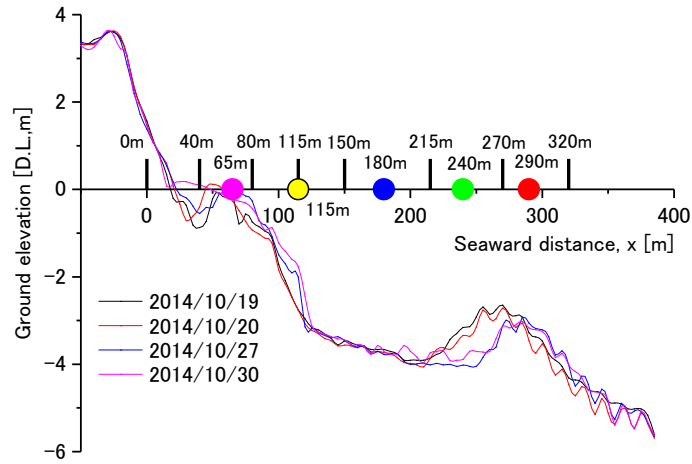


Figure 2. Seabed profile changes during the experiments.



Picture 1. Five colored fluorescent sand tracers. (a) pink, (b) yellow, (c) blue, (d) green, and (e) red.

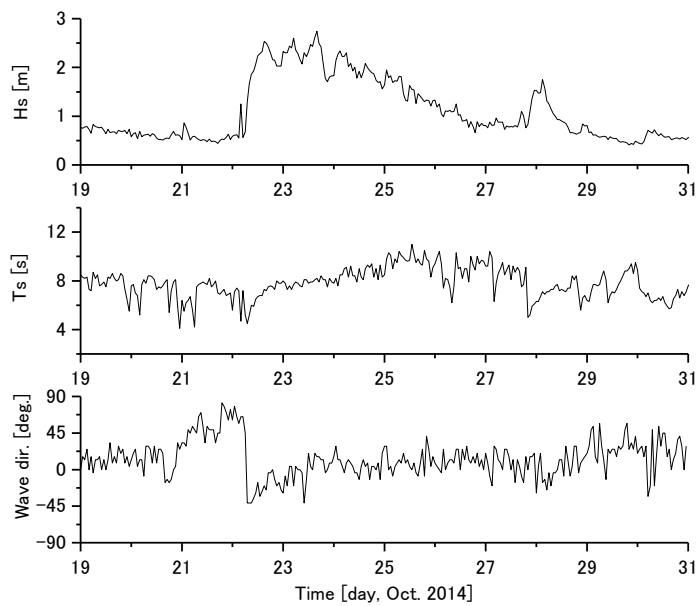


Figure 3. Observed time series data during the experiments. (a) significant wave height, (b) significant wave period, and (c) wave direction.

Clear acrylic pipes with an inner diameter of 52 mm and a length of 1.3 m were used to collect the core samples. The sampling locations were set along the profile of where the fluorescent sand was installed at $x = 0$ m, 40 m, 80 m, 115 m, 150 m, 215 m, 270 m, and 320 m, as indicated by the solid vertical lines shown in Fig. 2. Table 1 shows the length of each core sample and the number of subdivided samples taken from each core. The core, which sampled at $x = 0$ m, was taken from the shore, while all other cores were taken from the seabed. The average core length for each offshore sampling point, i.e. taken from the seabed, was 43.7 cm (Picture 2).

Each core was scanned with an X-ray CT system (LightSpeed Ultra16GE, GE Healthcare Japan Co. Ltd.) to understand the sediment accumulation profile and subsequent laminar plane. The dark-colored areas of the images captured by the scanner denote a high-density, whereas light-colored areas suggest a low density. After an initial scan, the core samples were cut vertically to view the accumulation profile and then subdivided into 5 cm segments. The cut surface of the sand core was scanned by a scanner. Each sample was then analyzed to determine the particle size distribution of the sediment core, the sieving and uniformity coefficients, and the number of fluorescent sand tracer particles per subdivided sample.

The fluorescent sand tracer particles were counted as indicated by their reactivity upon exposure to black light with respect to each subdivided sample. Also, the particle size distribution of the sediment for each subdivided sample was measured and analyzed by using an automated sonic sieving particle size analyzer robot sifter (RPS-205, Seishin Ent. Co. LTD).

Table 1. Outline for each core.

Location, x [m]	0	40	80	115	150	215	270	320
Length of each core [cm]	77	40	50	42	52	30	46	46
Number of subdivided samples	17	8	12	9	12	8	10	11



Picture 2. Collected vertical core samples.

3. Results of vertical distribution of core samples at each location

The vertical distribution of the observed sediment characteristics was analyzed to display the information in a number of forms for each core sample including (a) an X-ray CT picture, (b) a graphic representation of the stratigraphic column, (c) a median diameter profile, (d) a profile of the sieving and uniformity coefficients, and (e) a profile of the number of fluorescent sand tracer grains detected in each subdivided sample. These vertical distributions were developed for each cross-shore sample. The red lines in each stratigraphic column indicate the locations of the lamina planes, and the blue horizontal lines indicate the seabed surface level for each day.

3.1. Cross-shore location of $x = 0$ m

The observed vertical distributions for the core sample taken at $x = 0$ m are shown in Fig. 4. This sample point is located in the swash zone and when the core was sampled there was no water covering the surface.

Coarse sand (particle diameter > 0.5 mm) was observed at depths of less than 10 cm and greater than 70 cm. In the upper layer (sample depth < 10 cm), the sieving coefficient was found to be approximately 3.0. This indicates that various particles diameters of sediment are mixed in this layer. Pink (installed at $x = 65$ m) and yellow (installed at $x = 115$ m) fluorescent sand tracers were found up to a depth of 20 cm. The yellow tracers were transported from more than 100 m offshore. Some tracers were found at a depth lower than the deepest observed ground surface level, observed on Oct. 27. Thus, it can be seen that during the storm the beach was eroded by at least 20 cm depth and accumulation of sand occurred after the storm.

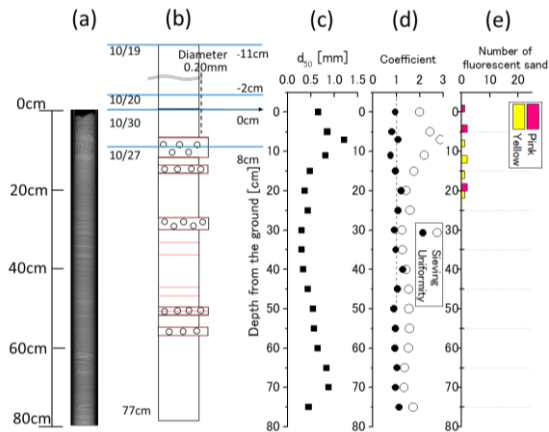


Figure 4. Vertical distributions of the sand core collected at $x = 0$ m. (a) X-ray CT picture (b) stratigraphic column, (c) median diameter, (d) sieving and uniformity coefficients, and (e) the number of fluorescent sand tracers.

3.2. Cross-shore location of $x = 80$ m

The observed vertical distributions of the core sample taken at $x = 80$ m are shown in Fig. 5. A coarse sand layer can be seen from 23 cm to 30 cm in depth. In this band, the sieving coefficient is larger than 1 and the uniformity coefficient is less than 1. Only pink (installed at $x = 65$ m) and yellow (installed at $x = 115$ m) fluorescent sand tracers were detected at this sample point. This indicates that even after the sediment movement due to the storm, sediment moved within the regions between the swash zone and surf zone. Moreover, since tracers were collected from the bottom layer of the core sample, more than 50 cm of sand was eroded and accumulated at this sample point.

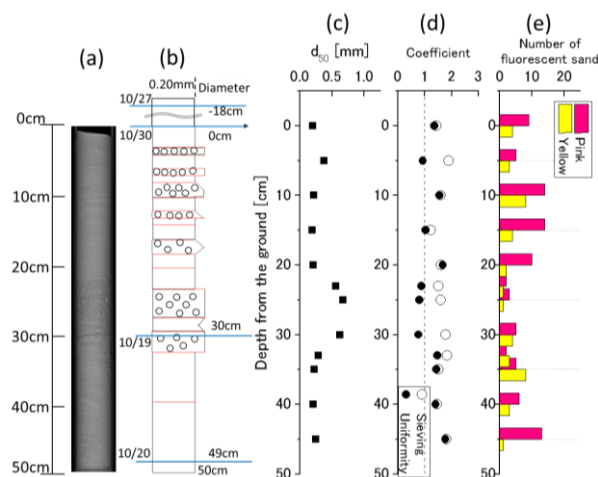


Figure 5. Vertical distributions of the sand core collected at $x = 80$ m. (a) X-ray CT picture (b) stratigraphic column, (c) median diameter, (d) sieving and uniformity coefficients, and (e) number of fluorescent sand tracers.

3.3. Cross-shore location of $x = 115\text{ m}$

Figure 6 shows the observed vertical distributions of the core sample taken at $x = 115\text{ m}$. In this location, the sediment diameter was observed to be relatively uniform with an average diameter was 0.18 mm . The sieving and uniformity coefficients were also observed to be constant from the top to the bottom of the core sample. A smaller number of laminar plates were observed as compared to other sample points. Pink and yellow fluorescent sand tracers were detected at all depths, especially pink tracers, which were the most frequently detected tracer. The seabed level was eroded by 100 cm on Oct. 20 due to the storm. Since the seabed slope at this sample point was steep (Fig. 2), it is considered that sediment was transported from the onshore side of the sample point and accumulation occurred rapidly after the storm. As the sample point was located at the same site as the yellow tracer, it may appear that insufficient yellow tracers have been detected. This may be explained by the broad distribution of the yellow tracers due to the storm and that tracers accumulated rapidly at depths greater than that of the core sample.

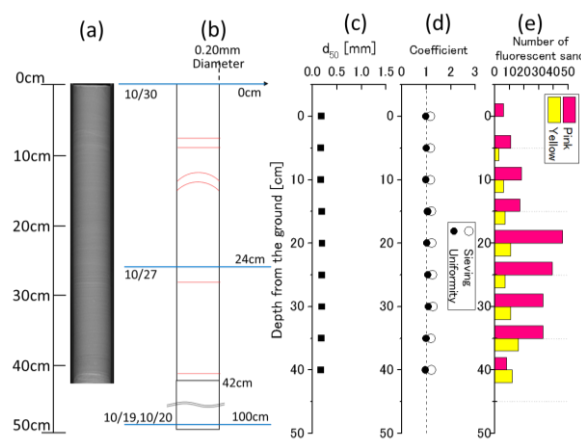


Figure 6. Vertical distributions of the sand core collected at $x = 115\text{ m}$. (a) X-ray CT picture (b) stratigraphic column, (c) median diameter, (d) sieving and uniformity coefficients, and (e) number of fluorescent sand tracers.

3.4. Cross-shore location of $x = 150\text{ m}$

Figure 7 shows the observed vertical distributions of the core sample taken at $x = 150\text{ m}$. This sample point was located at the onshore side of the trough region. Compared to other sample points, the seabed profile did not change significantly during the observation. Coarse sand was found uniformly to a depth of 40 cm

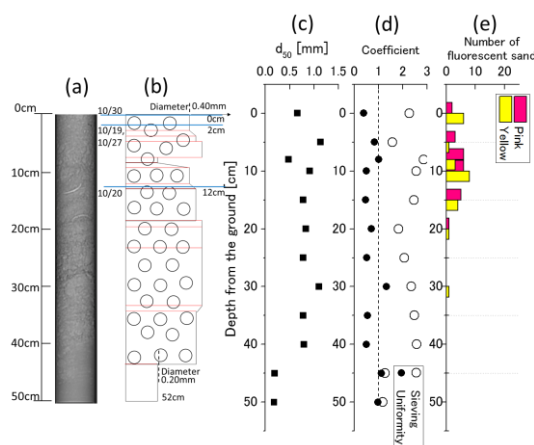


Figure 7. Vertical distributions of the sand core collected at $x = 150\text{ m}$. (a) X-ray CT picture (b) stratigraphic column, (c) median diameter, (d) sieving and uniformity coefficients, and (e) number of fluorescent sand tracer.

and the average diameter was 0.72 mm. In this band, the average sieving and uniformity coefficients are 2.30 and 0.68, respectively. This is the only sample point where coarse sand was observed to accumulate in the surface layer. At this sample point, onshore (pink and yellow) fluorescent sand tracers were detected, however, blue tracers (installed at $x = 180$ m), were not observed to accumulate here.

3.5. Cross-shore location of $x = 215$ m

Figure 8 shows the observed vertical distributions for the core sample taken at $x = 215$ m. Coarse sand layers were found at approximately 5 cm in depth and again at depths greater than 22 cm. In these layers, the average sieving coefficient was 1.72. In this core sample, pink and yellow tracers were detected, however, similar to a cross-shore location of $x = 150$ m, blue tracers (installed at $x = 180$ m) were not detected. As the pink tracer (installed at $x = 65$ m) was detected, it can be seen that the sand was transported offshore by a distance of at least 150 m.

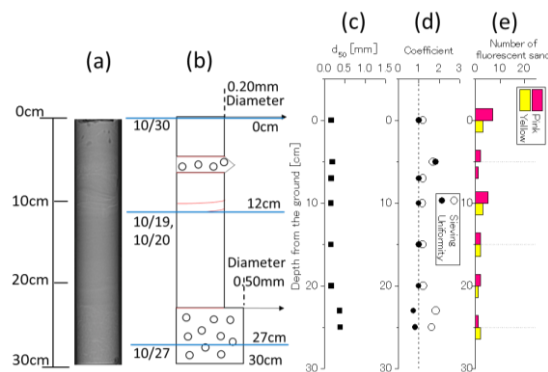


Figure 8. Vertical distributions of the sand core collected at $x = 215$ m. (a) X-ray CT picture (b) stratigraphic column, (c) median diameter, (d) sieving and uniformity coefficients, and (e) number of fluorescent sand tracers.

3.6. Cross-shore location of $x = 270$ m

The observed vertical distributions of the core sample at $x = 270$ m were taken from a sample point at the crest of the bar and are shown in Fig. 9. The green (installed at $x = 240$ m) and red (installed at $x = 290$ m) fluorescent sand tracers detected at this sample point were different to those collected at other locations in the onshore direction.

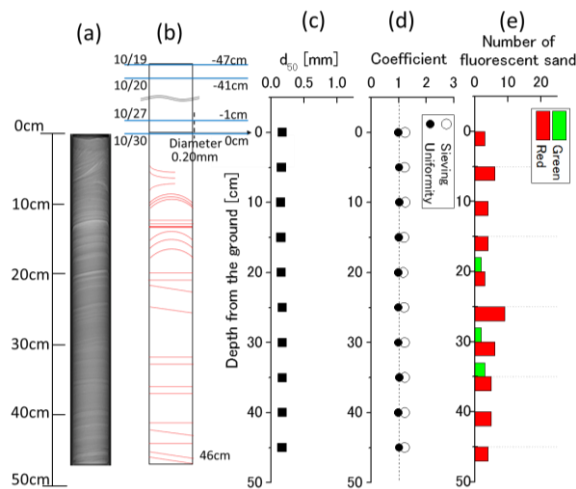


Figure 9. Vertical distributions of the sand core collected at $x = 270$ m. (a) X-ray CT picture (b) stratigraphic column, (c) median diameter, (d) sieving and uniformity coefficients, and (e) number of fluorescent sand tracers.

The average sediment diameter was observed to be 0.16 mm and the sieving and uniformity coefficients showed a nearly constant value of 1.21 and 1.00, respectively. Fluorescent sand tracers were detected at the bottom section of the core sample, thus, more than 90 cm of seabed erosion occurred during the storm and more than 46 cm of sediment accumulated at the sample point after the storm. In this core sample, more laminar planes were observed when compared to other core samples. Therefore, although the time scale was unknown, sediment accumulation occurred in an incremental manner.

4. Sediment Movements During a Storm

The sediment movement in the region between the swash zone to the offshore side of the bar can be characterized by Figures 10a, 10b, and 10c. They show the changes to the seabed profile, the differences in sediment volume during the observation period, and the spatial distribution of each different colored fluorescent sand tracer, respectively. The difference in sediment volume was calculated every 5 m in the cross-shore direction. The circles in Fig. 10a represent the installation locations of the fluorescent sand tracers and the vertical solid lines indicate the sample points where the sand cores were collected from. The length of the vertical solid lines corresponds to the length of the collected core (Table 1).

During the observation, sediment accumulation occurred in areas corresponding to an approximate cross-shore distance of $x = 35$ m and 110 m with 21.1 m^3 and 19.3 m^3 of sediment being deposited, respectively. In contrast, sediment erosion occurred in an area at an approximate cross-shore distance of $x = 255$ m, where 34.1 m^3 of sediment was eroded.

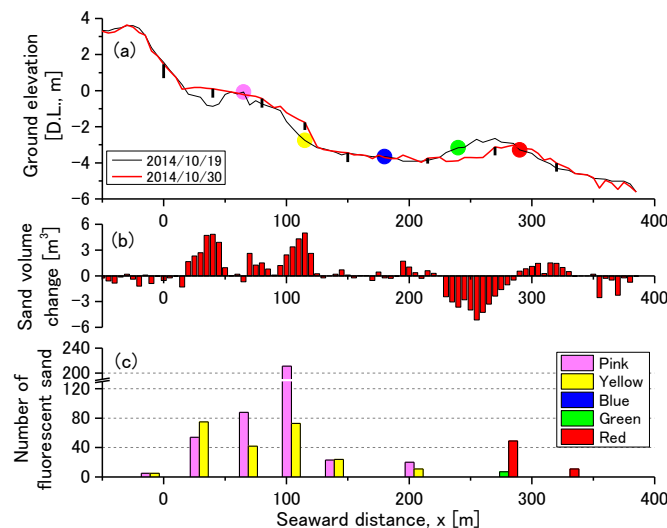


Figure 10. (a) Beach profile change, (b) sediment volume difference during the experiment, and (c) spatial distribution of the number of fluorescent sand tracers.

From Fig. 10c it can be shown that the pink tracer (installed at $x = 65$ m) and the yellow tracer (installed at $x = 115$ m), were both found in the same cross-shore region from $x = 0$ m to 215 m, based on the number of fluorescent sand tracers found at each sample point. According to barycentric positions of both colors, the dominant moving directions for pink and yellow tracers were offshore and onshore wards, respectively. It can be considered that transported offshore was due to an undertow until just before they reached the location of the bar and transported onshore was due to the bed load. Furthermore, as a large number of pink tracers were found at $x = 115$ m, whereas green and red tracers were not, sediment accumulation in this area is considered to have occurred due to sediment movement in the surf zone.

The blue fluorescent sand tracers that were installed at the trough region, $x = 180$ m, were not detected in any of the core samples. They were neither in the surf zone nor the swash zone. The blue tracers were installed in the trough region. There is a possibility that these tracers were transported in the longshore direction due to a rapid longshore current present during the storm event, but no cross-shore movement of

these tracers was detected.

A small number of the green tracers installed at $x = 240$ m were found only at the core sample taken at $x = 270$ m. They are considered to have been advected in the longshore direction, similar to the blue tracers. The red tracers, which were installed at the offshore side of the bar, $x = 320$ m, were found at $x = 270$ m and 320 m.

The cross-shore distribution of the longshore current was relatively large at the onshore side of the bar and has been observed to become smaller at the offshore side of the bar (Kuriyama, 2010). This may explain why the red tracers accumulated relatively close to the location where they were installed, unlike the blue or green colored tracers.

At a cross-shore location of $x = 245$ m on the upward seabed slope of the onshore side the bar, the instrument array was installed. The array consisted of a wave gauge (Infinity-WH, JFE Advantec Co., Ltd.) and a current meter (Infinity-EM, JFE Advantec Co., Ltd.). The observation point of the current meter was 0.7 m above the seabed when it was installed on Oct. 19. Due to the seabed profile changing because of the storm, however, the array fell down on Oct. 24 at 7:50 am. Figure 11 shows the observed data of the cross-shore and longshore current velocities at $x = 245$ m. The instrument array recorded the current velocity using two-minute averaged values every ten minutes. The positive values for the cross-shore and longshore current velocity refer to the landward and southward directions (Fig. 1), respectively.

The longshore current velocity was observed to increase with an increased wave height and the direction of the longshore current velocity changed from southward to the northward during the storm event. The longshore current, which occurred at the trough area, was shown to significantly affect sediment movement in this region. Before the high waves were generated by the storm event, the longshore current velocity was also small and change in the seabed profile was minor. At this stage, the fluorescent sand tracers remained close to their installation locations, especially at sample points greater than $x = 100$ m offshore. However, once the storm impacted the beach, the sand tracers were advected.

Kuriyama (2010) developed a one-dimensional parametric model for undertow and longshore current velocities. This model consists of three sub-models for wave transformation, undertow velocity and longshore velocity. By using this model, the longshore current velocity during the observations could be calculated. The model outputs for longshore current velocity every hour are shown in Fig. 11 as indicated by the square solid line. From these results, it can be shown that during the storm event between Oct. 22 and Oct. 24, the longshore current velocity initially tended northward at approximately 0.5 m/s, before changing direction and tending southward on Oct. 23 at a velocity of 0.7 m/s.

While short-term seabed profile changes, such as those brought about by a storm event, are generally thought to be caused by cross-shore sediment transport, the results from this study suggest that longshore sediment transport also impacts this process, based on the seabed profile and shape of the bar.

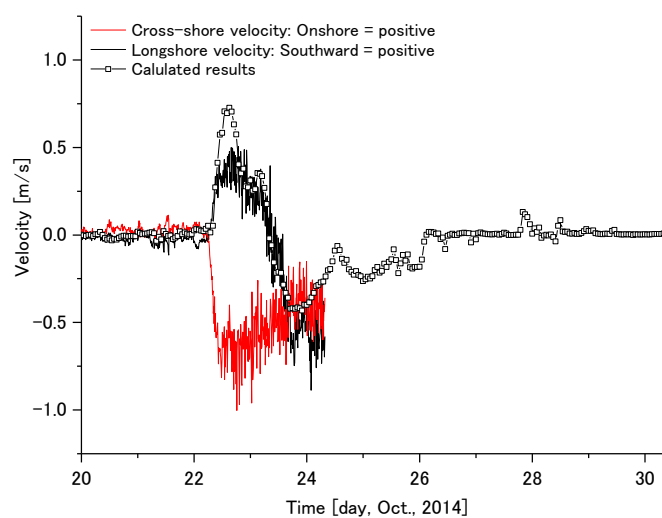


Figure 11. Observed and calculated results of current velocities at $x = 245$ m.

5. Conclusions

Field observations were conducted on the Hasaki coast in Japan and sediment movements during a storm were analyzed using fluorescent sand tracers. Five different colored fluorescent sand tracers were installed at points from near to the shoreline to the offshore side of the bar, and eight cores were sampled 12 days after the tracers were installed. A beach profile survey was conducted four times and wave data were observed as part of the methodology. Overall it was found that:

- 1) Sediment movements could be distinguished based on their relative cross-shore location of the sediment cores, with respect to the bar. Moreover, sediment transport in trough areas during a storm event is strongly affected by longshore currents.
- 2) Sediment erosion and accumulation is a common characteristic of storm events; however, even when similar thicknesses of sediment accumulation have occurred, the accumulation process is highly dependent on the cross-shore and longshore location of the activity.
- 3) By using not only the beach profile data but also the core sampling data and fluorescent sand tracers, the cross-shore sediment transport movements and the vertical sediment mixing during the storm event could be analyzed.

Acknowledgments

The authors would like to thank the Marine Information Division, Port and Airport Research Institute and Kashima Port and Airport Construction Office for allowing the use of wave data from the Port of Kashima. Also, authors would like to thank Prof. Yoshiyuki Nakamura and Dr. Hiroto Higa of Yokohama National University for their helpful comments. This research was funded through a JSPS Grant-in-aid for Young Scientists (A), No. 26709034. Furthermore, the authors gratefully acknowledge the Kochi Core Center, Japan (14B051) for the use of their facilities.

References

- Ciavola, P., Taborda, R., Ferreira, O. and Dias, J.A., 1997. Field observations of sand-mixing depths on steep beaches, *Marine Geology*, 141, 147-156.
- Inman, D.L., Zampol, J.A., White, T.E., Hanes, D.M., Waldorf, B.W. and Kastens, K.A., 1980. Field measurements of sand motion in the surf zone, *Coastal Engineering Proceedings*, 1(17), doi:http://dx.doi.org/10.9753/icce.v17.%p.
- Jolliffe, I.P., 1963. A study of sand movements on the Lowestoft sandbank using fluorescent tracers, *Geographical Journal*, 129, 480-493.
- Kaczmarek, L.M., Biegowski, J. and Ostrowski, R., 2004. Modelling cross-shore intensive sand transport and changes of bed grain size distribution, *Coastal Engineering*, 51, 501-529.
- Katoh, K. and Tanaka, N., 1986. Local movements of sand in the surf zone, *Coastal Engineering Proceedings*, 1(20), doi: http://dx.doi.org/10.9753/icce.v20.%p.
- Katoh, K., Yanagishima, S., Kuriyama, Y., Isogami, T., Murakami, H. and Fujita, M., 1990. Change of the grain distribution of bed material in the surf zone, Report of PHRI, 29 (2), 37-61 (in Japanese).
- Katoh, K. and Yanagishima, S., 1995. Changes of sand grain distribution in the surf zone, *Coastal Dynamics' 95*, 639-650.
- Kennedy, V.C. and Kouba, D.L., 1970. Fluorescent sand as a tracer of fluvial sediment, *Professional Paper USGS*, 562E.
- Kraus, N.C. and Smith, J.M., 1994. SUPERTANK laboratory data collection project, *Technical report CERC-94-3*. 285p.
- Kuriyama, Y., 2002. Medium-term bar behavior and associated sediment transport at Hasaki, Japan, *J. Geophysical Res.*, 107 (C9), 3132, doi:10.1029/2001JC000899.
- Kuriyama, Y., 2010. A one-dimensional parametric model for undertow and longshore current velocities on barred beaches, *Coastal Engineering Journal*, 133-155, DOI No: 10.1142/S0578563410002130.
- Tonk, A. and Masselink, G., 2005. Evaluation of longshore transport equations with OBS sensors, streamer traps, and fluorescent tracer, *Journal of Coastal Research*, 21(5), 915-931.
- Masselink, G., Auger, N., Russell, P. and O'Hare, T., 2007. Short-term morphological change and sediment dynamics in the intertidal zone of a macrotidal beach, *Sedimentology*, 54, 39-53.
- Williams, J.J., Buscombe, D., Masselink, G., Turner, I.L. and Swinkels, C., 2012, Barrier dynamics experiment (BARDEX): Aims, design and procedures, *Coastal Engineering*, 63, 3-12.

Yamada, F., Tateyama, R., Tsujimoto, G., Sueenaga, S., Long, B. and Pilote, C., 2013. Dynamic monitoring of physical models beach morphodynamics and sediment transport using X-ray CT scanning technique, *Journal of Coastal Research*, SI, 65, 1617-1622.